PAIN® 151 (2010) 655–663

PAIN®

www.elsevier.com/locate/pain

Assessment of brain responses to innocuous and noxious electrical forepaw stimulation in mice using BOLD fMRI

Simone C. Bosshard [a], Christof Baltes [a], Matthias T. Wyss [b,c], Thomas Mueggler [a], Bruno Weber [b], Markus Rudin [a,b,*]

[a] Institute for Biomedical Engineering, University and ETH Zurich, Switzerland
[b] Institute of Pharmacology and Toxicology, University of Zurich, Switzerland
[c] PET Center, Department of Nuclear Medicine, University Hospital Zürich, Switzerland

ARTICLE INFO

Article history:
Received 27 November 2009
Received in revised form 4 August 2010
Accepted 17 August 2010

Keywords:
Mouse fMRI
Electrical forepaw stimulation
BOLD signal
Somatosensory cortex

ABSTRACT

Functional magnetic resonance imaging (fMRI) using the blood oxygen level-dependent (BOLD) contrast was used to study sensory processing in the brain of isoflurane-anesthetized mice. The use of a cryogenic surface coil in a small animal 9.4*T* system provided the sensitivity required for detection and quantitative analysis of hemodynamic changes caused by neural activity in the mouse brain in response to electrical forepaw stimulation at different amplitudes. A gradient echo-echo planar imaging (GE-EPI) sequence was used to acquire five coronal brain slices of 0.5 mm thickness. BOLD signal changes were observed in primary and secondary somatosensory cortices, the thalamus and the insular cortex, important regions involved in sensory and nociceptive processing. Activation was observed consistently bilateral despite unilateral stimulation of the forepaw. The temporal BOLD profile was segregated into two signal components with different temporal characteristics. The maximum BOLD amplitude of both signal components correlated strongly with the stimulation amplitude. Analysis of the dynamic behavior of the somatosensory 'fast' BOLD component revealed a decreasing signal decay rate constant k_{off} with increasing maximum BOLD amplitude (and stimulation amplitude). This study demonstrates the feasibility of a robust BOLD fMRI protocol to study nociceptive processing in isoflurane-anesthetized mice. The reliability of the method allows for detailed analysis of the temporal BOLD profile and for investigation of somatosensory and noxious signal processing in the brain, which is attractive for characterizing genetically engineered mouse models.

1. Introduction

Processing of noxious stimuli involves different levels and structures of the neural system. In spite of substantial progress in understanding the molecular mechanisms underlying pain, many aspects are still poorly understood. Genetically engineered mouse lines displaying altered or pathological pain states may help to elucidate the physiological and molecular basis of normal and pathological pain processing [7,17,21,34]. Classically, sensory responsiveness in animals is characterized using behavior tests such as the hot plate, von Frey filaments or tail flick test [54]. These analyses, however, depend on the skills of the experimenter and require undisturbed motor function of the animal. Electrophysiological recordings of neuronal activity provide high spatial and temporal resolution. However, the method is invasive and does not allow recording signals over extended brain areas in a limited time period. An objective readout of neuronal signal processing that is non-invasive, independent of the observer performance and capable of covering the entire brain would be highly desirable. Functional magnetic resonance imaging (fMRI) has been widely used to assess changes in brain activity evoked by noxious stimuli. Noxious-evoked activation patterns revealed by fMRI correspond well with the structures of the pain-processing pathway both in humans and animals [6,11,26,28,30]. There are two peripheral nerve types which process sensory input: low threshold fibers, mainly Aβ, primarily mediate touch, while high threshold fibers, mainly Aδ and C, conduct nociceptive signals [8]. The response to peripheral sensory or noxious stimulation in rats has been studied in depth [23,24,39]. In contrast, only few fMRI studies in mice using electrical stimulation paradigms have been reported to date [1,2,31,33]. This is mainly due to experimental challenges related with the small size of mice, putting high demands on spatial resolution and thus sensitivity. Another challenge for robust fMRI

* Corresponding author. Address: Animal Imaging Center – ETH Zurich, Wolfgang-Pauli-Str. 27, CH-8093 Zürich, Switzerland. Tel.: +41 44 633 76 04 (HIT E22.4), +41 44 633 76 73 (HIT E22.2); fax: +41 44 633 11 87.
E-mail address: rudin@biomed.ee.ethz.ch (M. Rudin).

0304-3959/$36.00
doi:10.1016/j.pain.2010.08.025

measurements in mice is the maintenance of stable physiological conditions. While human fMRI experiments are carried out in awake subjects, the large majority of animal fMRI studies are performed in anesthetized animals. Therefore, anesthesia should neither interfere with brain activity nor act analgesic when investigating the response to noxious stimulation paradigms. Unfortunately, there is no such ideal anesthetic suitable for longitudinal studies e.g. for studying functional changes over time. In this work we used isoflurane, the advantages of which are ease of administration and controlled dosing. Despite these challenges, the development of robust mouse fMRI protocols is highly desirable for investigating mechanistic aspects of signal processing under normal and pathological conditions.

The aim of this study was to develop a reliable stimulation paradigm to analyze the somatosensory and nociceptive system in mice under isoflurane anesthesia. The high sensitivity of a cryogenic surface coil enabled detailed analysis of the BOLD response in activated brain regions elicited by electrical stimulation of the mouse forepaw as a function of time. BOLD signal intensities were found to correlate well with the amplitudes of the electrical stimulation applied. The quantitatively assessed dynamics of the temporal profile of the BOLD response yielded further insight into the hemodynamic response to electrical stimulation.

2. Materials and methods

2.1. Animal preparation

All experiments were performed in accordance with the Swiss law of animal protection. 15 female C57Bl/6 mice weighing 22 ± 3 g were anesthetized with Isoflurane (induction 2–3%, maintenance 1.2% in a 70% air – 30% oxygen mixture; Abbott, Cham, Switzerland), endotracheally intubated and mechanically ventilated throughout the experiment to ensure stable physiology (90 breaths/minute, respiration cycle: 25% inhalation, 75% exhalation; Maraltec, Alfos Electronics, Biel-Benken, Switzerland). Animals were paralyzed by intravenous (i.v.) administration of a neuromuscular blocking agent (Pancuronium bromide, 1.0–1.5 mg/kg; Sigma-Aldrich, Steinheim, Germany), which avoided interference by spontaneous breathing and prevented movement artifacts during the fMRI experiments despite the low isoflurane levels. A rectal temperature probe (MLT415, AD Instruments, Spechbach, Germany) was inserted to keep the animal at 36.5 ± 0.5 °C. Body temperature was maintained using a warm-water circuit integrated into the animal support (Bruker BioSpin AG, Fällanden, Switzerland). A transcutaneous electrode (TCM4, Radiometer, Copenhagen, Denmark) was placed on the shaved upper hind limb of the mouse to measure blood gas levels (pCO_2). In some animals, heart rate and blood oxygenation were monitored using a MR-compatible infrared sensor (MouseOx® Pulse Oximeter, Starr Life Sciences, Oakmont, PA, USA). For accurate and reproducible positioning, the head of the animals was fixed with stereotactic ear bars and eye cream was applied to prevent the eyes from becoming dry. For the electrical stimulation a pair of needle electrodes (Genuine Grass instruments, West Warwick, USA) was inserted subcutaneously into the distal and proximal end of the palm of each forepaw with a distance of 2–3 mm between the two needles. The identical setup and parameters (1.5 mA) were used to stimulate the hind paw of four animals.

The entire experiment lasted approximately 2 hours, of which 20 min were used for preparation of the mouse, and the remaining time was used for acquiring fMRI data. The mice were anesthetized throughout the experiment. Animals were used for more than one experiment.

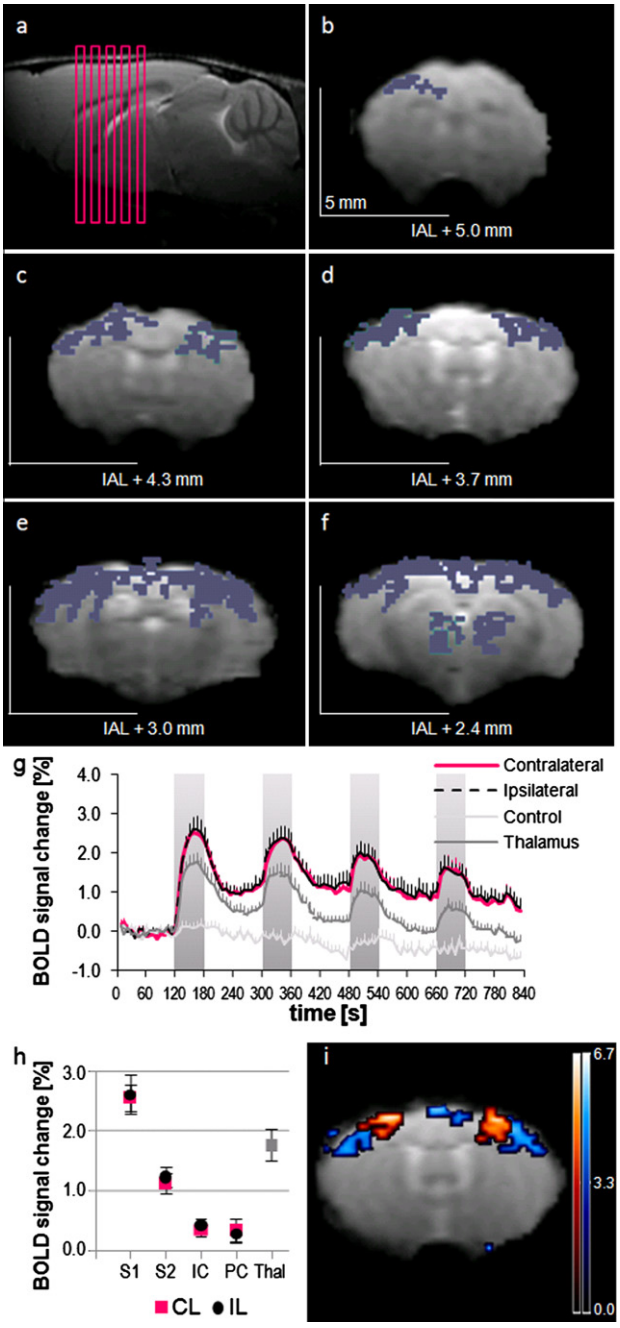

Fig. 1. Spatial distribution of the BOLD activation. (a) Sagittal reference image indicating the positions of the coronal EPI slices covering a large section of the mouse forebrain. (b)–(f) Spatial distribution of the activated clusters ($p = 0.0001$) of one representative animal after unilateral forepaw stimulation. The left side of the image corresponds to the left hemisphere. Nominal distance to the interaural line (IAL) is given for each slice. Scale bar indicates 5 mm. Activated areas include the S1 forelimb area (c–e); motor cortex M1 (c–e); and several nuclei of the thalamus, including the ventral posterior nucleus which relays somatosensory information (f). Activated clusters are also observed at the sagittal sinus (e, f). (g) Time course of the BOLD signal after unilateral electrical stimulation of the forepaw at 1.5 mA for S1 contralateral to the stimulated paw (pink), S1 ipsilateral (dashed black), thalamus (gray), and the control region (light gray). Gray bars indicate the stimulation periods. The BOLD signals of the contralateral and ipsilateral S1 are almost identical. (h) Maximal signal amplitude of different regions (S1, S2, insular cortex (IC), piriform cortex (PC, control region)) ipsi- (black circles) and contralateral (pink squares) to the stimulated paw at 1.5 mA. All values are given as mean + SEM. (i) Activation map of two representative animals showing activation of the forepaw (blue) and hind paw (red) S1 area after stimulation of the respective paw at 1.5 mA, overlaid on an EPI image. Scale bars indicate *t*-values.

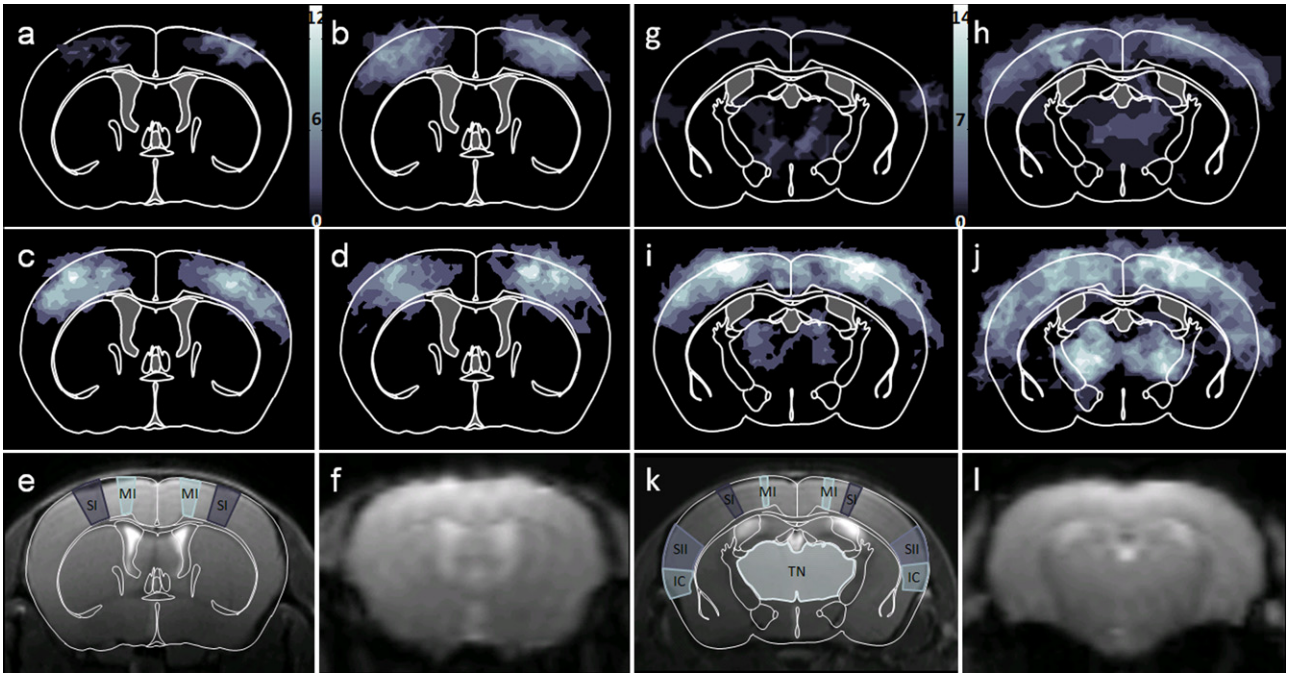

Fig. 2. Activation maps of the cortex after left and right forepaw stimulation at (a, g) 0.5 mA, (b, h) 1.0 mA, (c, i) 1.5 mA, (d, j) 2.0 mA. Data show activated clusters derived from GLM analysis ($p = 0.0001$, cluster size: 15 voxels) for all animals overlaid on the mouse brain atlas at IAL + 3.7 mm (a–f) and IAL + 2.8 mm (g–l) [13]. (e–k) Mouse brain atlas with relevant regions (SI: primary somatosensory cortex, forepaw region; SII: secondary somatosensory cortex; IC: insular cortex; MI: primary motor cortex; TN: thalamic nuclei) overlaid on the anatomical image. (f, l) Representative EPI image revealing relatively little distortions. (g–j) Activation maps; intensity indicates the number of stimulation periods displaying significant BOLD activation at a given location (scale bar).

2.2. MRI equipment and sequences

All MRI experiments were performed on a Bruker BioSpec 94/30 small animal MR system (Bruker BioSpin MRI, Ettlingen, Germany) operating at 400 MHz (9.4 Tesla). For signal transmission and reception a commercially available cryogenic quadrature RF surface probe (CryoProbe), consisting of a cylinder segment (180° coverage, radius = 10 mm) and operating at a temperature of 30 K was used (Bruker BioSpin AG, Fällanden, Switzerland) (for detailed information see [3]). The ceramic outer surface of the coil touching the mouse head was kept at 30 °C using a temperature-controlled heating device.

Anatomical reference images in coronal and sagittal directions (slice orientations are given using the nomenclature of the mouse brain atlas [13]) were acquired using a spin echo (Turbo-RARE) sequence with the following parameters: field-of-view (FOV) = 20 × 20 mm^2, matrix dimension (MD) = 200 × 200, slice thickness (STH) = 0.5 mm, interslice distance (ISD) = 1.0 mm, repetition delay T_R = 3500 ms, echo delay T_E = 13 ms, effective echo time $T_{E,eff}$ = 39 ms, RARE factor (number of echoes sampled for each excitation) = 32, and number of averages (NA) = 1. Subsequently, the slices for the fMRI experiment were planned on the anatomical reference image and BOLD fMRI data were acquired using a gradient-echo-echo planar imaging (GE-EPI) sequence with the following parameters: Five coronal slices covering a range of 2 to 5 mm anterior to the interaural line were recorded with FOV = 23.7 × 12.0 mm^2, MD = 90 × 60 (acquisition) and 128 × 64 (reconstruction) yielding an in-plane resolution of 200 × 200 μm^2, STH = 0.5 mm, ISD = 0.7 mm, T_R = 2500 ms, T_E = 8.5 ms, and NA = 3 resulting in an image acquisition time of 7.5 seconds. The individual sections comprised the forelimb and hind limb areas of the somatosensory and insular cortices, and the thalamus [13]. An

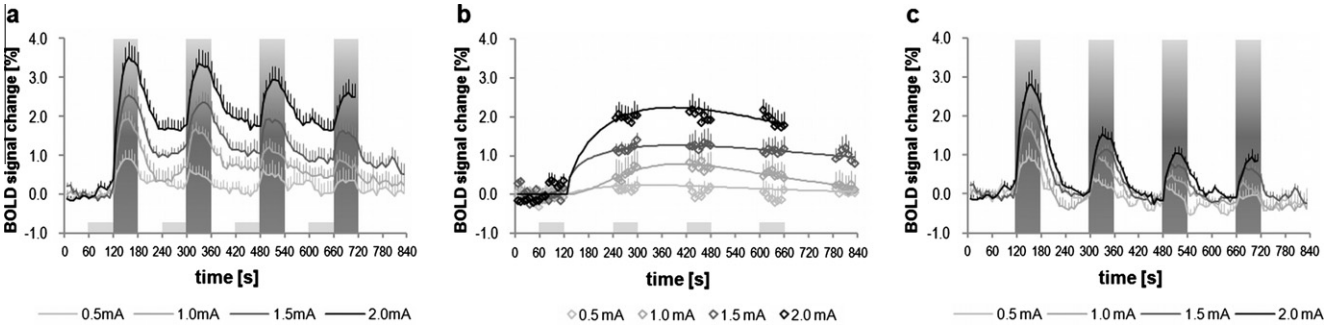

Fig. 3. (a) Relative change of the BOLD signal intensity as a function of time during electrical forepaw stimulation for the different stimulation amplitudes. Dark gray bars indicate the stimulation periods, light gray boxes mark data points used for fitting the component *S* curve (b). (c) Signal component *F* obtained by subtracting (b) from (a). Values are given as mean + SEM.

fMRI experiment consisted of 112 repetitions and lasted 14 min, except for the group of 2.0 mA, where the acquisition consisted of 96 repetitions and lasted 12 min.

2.3. Electrical stimulation paradigm

Electrical pulses of 0.5 ms duration at a frequency of 3 Hz were applied. Current amplitudes were 0.5 mA ($n = 8$ animals), 1.0 mA ($n = 8$), 1.5 mA ($n = 7$), and 2.0 mA ($n = 8$) [42]. The stimulus strength is determined by the local current density (electric current per unit area of cross section), which itself depends on the placement of the electrodes. Current thresholds for noxious stimulation were estimated from an experiment on the hairy skin of the wrist of a volunteer with analogous electrode placement as in mice (distance between electrodes). Stimulation amplitudes of 1.5 and 2.0 mA were experienced as being painful, while the amplitude of 0.5 mA was clearly innocuous. Although innervation of human and mouse skin may differ, a noxious threshold in the range of stimulation amplitude of 1.0 mA appears reasonable.

The stimulation paradigm consisted of a block design starting with a resting period of 120 seconds (baseline) followed by 60 seconds of stimulation. This series was repeated four times and fMRI data recording was continued for another 120 seconds after the last stimulation block. The duration between positioning of the mouse in the magnet bore and the beginning of the electrical stimulation and fMRI recording was kept constant at 40 minutes to ensure the same anesthesia conditions for all animals. This time was used for adjustment of MRI conditions as well as anatomical reference and high resolution scans. Stimulation started with the left paw in all animals. Following an 8 minute resting interval, the right paw was stimulated. These two stimulation cycles were followed by a control acquisition without electrical stimulation.

2.4. Data analysis

Four regions of the brain were evaluated in detail, including the somatosensory cortex S1 contralateral and ipsilateral to the stimulated paw, the thalamus and a control region at the ventral pallidum, a structure involved in neither the sensory nor the nociceptive pathway. In addition, we looked at the S2, insular and piriform cortex in the 1.5 mA group. Statistical t-maps were calculated using the general linear model (GLM) tool integrated in the Biomap software program (M. Rausch, Novartis, Switzerland). GLM assesses correlations on a pixel-by-pixel basis between the fMRI signal train and the stimulation paradigm. Activation was detected using a statistical threshold of $p = 0.0001$ for all experiments. With a minimal cluster size of 15 voxels, two coronal sections were analyzed, of which one slice covered the thalamus, the secondary somatosensory (S2) and insular cortex (IC) (2.8 mm anterior to the interaural line (IAL + 2.8 mm)) and the other covered the forepaw areas of the primary somatosensory cortex (S1) (IAL + 3.7 mm). The respective regions-of-interests (ROIs) derived from the GLM analysis were used to extract BOLD signal changes as a function of time. In cases for which the correlation analysis revealed no activated voxels at the expected locations as well as for the unstimulated scans ROIs were transferred from the mouse brain atlas [13]. For group analysis, EPI images covering the S1 area (IAL + 3.7 mm) and the thalamus (IAL + 2.8 mm) were normalized to the coordinate system of the mouse brain atlas [13]. The fMRI coordinates were defined as followed: the origin of the right-hand coordinate system was chosen at the ventral end of the brain midline through the coronal sections. The second reference point was the dorsal end of the same midline, while the third point was placed on the edge of the right hemisphere at its widest point. The coordinate axes were defined along the midline (y-axis) and perpendicular to it (x-axis). The axes were then scaled to fit the dimensions of the mouse brain atlas, using an IDL-based software developed in-house [48].

For a detailed analysis of the fMRI time curve, the resulting BOLD profile was segregated into two components S ('slow') and F ('fast'). Component S was extracted by fitting the 8 data points before stimulation onset (light gray bars, shown in Fig. 3a, b) to a gamma-variate function: $y(t) = a \times t^r \times \exp(-k \times t)$ with a (amplitude factor), r (power of growth curve), k (rate of exponential decay) being the parameters to be optimized, while t is measured with regard to the start of the first stimulation period ($t = 0$). The best fit curve (solid line, Fig. 3b) was then subtracted from the original data to yield component F of the fMRI signal (Fig. 3c). The maximal amplitudes of the fitted curve for component S and of the extracted curve for the first stimulation period of component F (see Fig. 3) were analyzed as a function of the stimulation amplitude. The quantitative analysis was carried out for all ROIs.

We furthermore analyzed the rates of BOLD signal increase and decay for both the first stimulation cycle and the entire stimulation period. The data points of the signal decay at the end of the stimulation interval (indicated by the dotted line in Fig. 5a) were used to calculate a decay constant k_{off} assuming a single exponential decay function, $S(t) = S(t = 0) \times \exp(-k_{off} \times t)$ with $S(t)$ indicating the signal amplitude during the decay at time t and $S(t = 0)$ the amplitude at the end of the stimulation period ($t = 0$). A minimum of four data points of the decay curve with an amplitude exceeding noise levels were required for each individual signal curve to allow for fitting. The BOLD signal decay rate constant was then correlated to the maximum BOLD response S_{max} of the single animals (Fig. 5c).

The constant k_{on} describing the initial build-up of the signal at the beginning of the stimulation to its maximum was calculated assuming the following relation: $S(t) = S_{max} \times [1-\exp(-k_{on} \times t/S_{max})]$ for which the initial slope yields $(\mathrm{d}s(t)/\mathrm{d}t_{t=0} = k_{on})$ i.e. the initial slope was assumed to be independent of the maximum BOLD signal.

2.5. Autoradiography and intrinsic optical imaging

Autoradiography with [^{18}F]-2-fluoro-2-deoxyglucose (^{18}F-FDG) was performed on two female C57Bl/6 mice according to published protocols [44,55]. The left forepaw was electrically stimulated at 1.5 mA using the parameters described above. A 5 minute stimulation period was followed by a 1 minute break. This was repeated for the entire time course of 45 minutes, before the animals were sacrificed and the brain extracted.

One mouse was used for intrinsic optical imaging. Reflectance from 570 nm light was measured through the exposed skull using a CCD camera. The left forepaw was stimulated with a 10 second pulse train of 0.5 msec pulses of 1.0 mA current amplitude at 3 Hz. These experiments were carried out under 1.5% isoflurane anesthesia.

3. Results

3.1. Animal physiology and anesthesia

Non-invasive monitoring of the mice showed stable physiology throughout the experiments. Blood gas levels of pCO_2 measured transcutaneously were in the range of 40 ± 10 mm Hg, which indicates a well-adjusted ventilation of the animals [50]. Body temperature was kept stable at 36.5 ± 0.5 °C for the entire experiment. The monitored heart rate was stable around 500 beats per minute in all animals and no changes were detected during the stimulation. After completion of the fMRI investigation, the animals recovered fast and could be used for further experiments, an important prerequisite for longitudinal studies.

3.2. Signal and image quality

By exploiting the significant gain in sensitivity provided by the use of a cryogenic RF surface coil for signal detection [35,3] BOLD fMRI data sets of high quality suitable for reproducible quantitative analysis have been obtained. Comparing the CryoProbe with a conventional room temperature coil of similar dimensions (for detailed information on the coils see [3]) using the GE-EPI sequence, a gain in image signal-to-noise ratio (SNR) of a factor of 3.1 ± 0.7 (mean ± standard deviation, unpublished data) was achieved. Using a coronal slice orientation proved advantageous as cross-sectional images recorded ⩾3 mm anterior to the interaural line were largely devoid of geometrical distortions caused by local magnetic field inhomogeneities due to different magnetic susceptibilities of adjacent tissue compartments. In caudal brain structures, significant susceptibility artifacts have been observed due to the proximity of the air-filled ear cavities. This also impaired the quality of images recorded in horizontal plane view, which would allow covering larger brain areas. Distortions caused by differences in susceptibility are experienced on an absolute scale, i.e. they affect more extended brain regions in mice than in rats due to the smaller dimensions of the mouse.

fMRI data showed good reproducibility (e.g. see error bars in Fig. 1 g, h) and allowed for assessing differences in the BOLD response during stimulation at different amplitudes.

3.3. Spatial distribution and intensity of the BOLD response

The spatial distribution of the activated areas after forepaw stimulation at 1.5 mA (threshold $p = 0.0001$, cluster size: 15 voxels) for one representative animal is shown in Fig. 1. The position of five coronal slices is indicated in the sagittal section shown in Fig. 1a. Besides the forepaw S1 region activated areas are present in other S1 areas (Fig. 1c–f), the primary motor cortex (Fig. 1c–f), and several nuclei of the thalamus, including the ventral posterior nucleus which relays somatosensory information to the cortex (Fig. 1f) [13]. Fig. 1i shows the distinction of the forepaw area (blue) and the hind paw area (red) after the respective stimulation as an activation map of two representative animals. As expected, hind paw somatosensory S1 areas were located median to the respective forepaw regions. The activated cluster at the brain midline reflects signal contributions from the sagittal sinus. No consistent deactivations were detected in any region of the brain.

Fig. 2 shows statistical maps (threshold $p = 0.0001$, cluster size: 15 voxels) depicted on the mouse brain atlas ([13], Fig. 2 a–f: IAL + 3.7 mm, Fig. 2 g–l: IAL + 2.8 mm) obtained from all animals at different stimulation amplitudes ((a, g) 0.5 mA, (b, h) 1.0 mA, (c, i) 1.5 mA, (d, j) 2.0 mA). The activated clusters of individual animals were overlaid, i.e. the intensity in the activation map corresponds to the number of animals displaying a significant BOLD signal (left and right forepaw for each animal). Activation in response to the forepaw stimulation appears in the somatosensory S1 and S2 cortices, in the thalamus and at higher amplitudes in the insular cortex (regions indicated in Fig. 2e, k). For all activated regions, the spatial extent of BOLD response exceeded the topological area defined on the basis of the mouse brain atlas [13]. This is attributed to the fact that fMRI assesses the hemodynamic response elicited by neural activity and not the neural activity per second.

3.4. BOLD signal changes in correlation to the forepaw stimulation paradigm

The maximal BOLD signal intensity increased with increasing stimulation amplitude in all analyzed regions involved in sensory and nociceptive processing in a comparable manner as in the regions shown in Figs. 3 and 4. Stimulation at the lowest amplitude of 0.5 mA led to a maximal BOLD signal of 0.93 ± 0.25% (in% of baseline intensity) in the primary somatosensory cortex contralateral to the stimulated paw. For amplitudes of 1.0, 1.5, 2.0 mA, the maximal BOLD signal changes in this region amounted to 1.94 ± 0.20%, 2.54 ± 0.22%, and 3.52 ± 0.41%, respectively (Fig. 3a). The maximum BOLD amplitude decreased for subsequent stimulation periods. Interestingly, the signal did not return to the initial baseline level within the two minutes resting interval following a stimulation episode, but stayed elevated until the start of the next stimulation block. The BOLD response to unilateral forepaw stimulation appeared consistently bilateral in all activated regions, including the S1 (Figs. 1 and 4), thalamus, S2 and insular cortex (for 1.5 mA: Fig. 1h). The maximal BOLD signal amplitude in the regions of the S2 somatosensory and insular cortex was significantly lower as compared to the S1 area. This was observed at all stimulation amplitudes except at 0.5 mA, where the amplitudes for S1 and S2 area reached similar values (data not shown). There was no delay between ipsi- and contralateral responses within the time scale of the fMRI experiment (7.5 s temporal resolution).

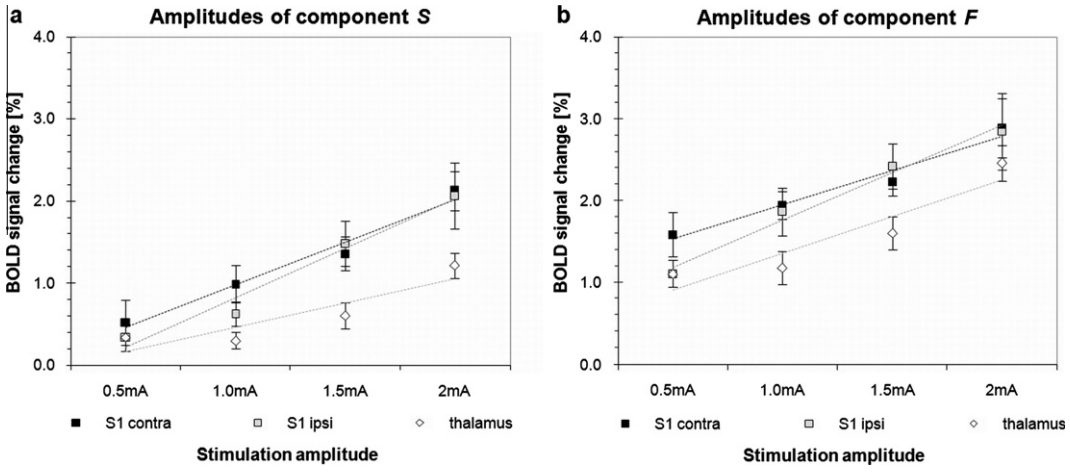

Fig. 4. The amplitudes of the two components S (a) and F (b) as a function of the stimulation amplitude. (a) Linear regression analysis yielded correlation factors of $R^2 = 0.98$ for the contralateral and $R^2 = 0.97$ for the ipsilateral S1 somatosensory cortical area. The corresponding value for thalamus was $R^2 = 0.81$. (b) For the fast component the correlation factors were: $R^2 = 0.97$ for contralateral S1, $R^2 = 0.98$ for ipsilateral S1 and $R^2 = 0.87$ for thalamus. Values are given as mean ± SEM.

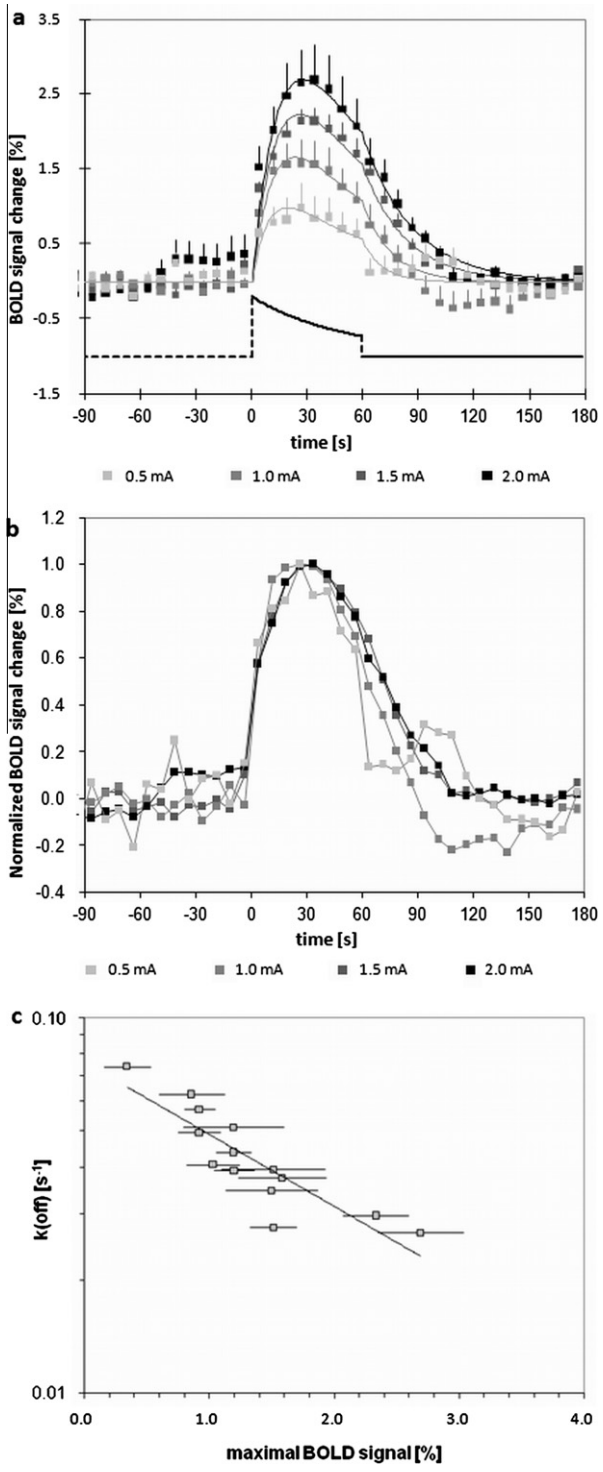

Fig. 5. Analysis of component *F* of the fMRI response to electrical stimulation of the forepaw in the contralateral S1 cortical region. (a) Mean fMRI signal response for the first stimulation episode as a function of time and current amplitude. Solid lines indicate the BOLD response modeled as described in the text. The dashed line illustrates the vasodilatory stimulus, which displays a single exponential decay with a rate constant $k_v = 0.02\ s^{-1}$. (b) The mean normalized fMRI response of the first stimulation period (normalized to one) as a function of time and stimulation amplitude. The reduced rate of signal decay with increasing stimulus amplitude (and correspondingly higher maximum BOLD intensity) becomes apparent. For sake of clarity error bars have been omitted. (c) The decay rate constant of the BOLD signal of the single animals decrease with increasing maximal intensity of the BOLD signal. Linear regression yielded a correlation coefficient of $R^2 = 0.76$. Values are given as mean ± SEM.

The control region, which was located in the ventral pallidum, a structure not involved in sensory or nociceptive processing, showed no change in BOLD intensity for stimulation amplitudes ⩽1.5 mA (Fig. 1g 1.5 mA). At 2.0 mA a maximum signal increase of 0.81 ± 0.12% was detected. This unspecific increase in the BOLD signal was observed in large parts of the brain. A second cortical control region, located in the piriform cortex, behaved comparable to the ventral pallidum (for 1.5 mA: Fig. 1h). No region-specific activation whatsoever, but only background noise was revealed by the analysis of the control fMRI data sets acquired without stimulation, indicating the stability of the fMRI setup including the physiological preparation (data not shown).

3.5. Amplitudes of the two signal components S and F as a function of the stimulation amplitude

The temporal profile of the BOLD response has been segregated into the two signal components *S* and *F* by fitting component *S* to a gamma-variate function and subtracting the best fit from the experimental data (Fig. 3b, c). Analysis of the maximal amplitude of both components for the two S1 regions and the thalamus was found to correlate with the stimulation amplitude. Linear regression analysis yielded correlation factors for component *S* (Fig. 5a) of $R^2 = 0.98$ for the contralateral, $R^2 = 0.97$ for the ipsilateral somatosensory cortex and $R^2 = 0.81$ for the thalamus. The values for component *F* (Fig. 5b) were $R^2 = 0.97$ for contralateral S1, $R^2 = 0.98$ for ipsilateral S1 and $R^2 = 0.87$ for thalamus.

3.6. Analysis of the signal dynamics of component F

Not only the amplitude but also the dynamic behavior of the BOLD response depended on the stimulation amplitude as demonstrated by the averaged temporal profile of component *F* of the first stimulation period of each animal (Fig. 5a). The maximum values for the S1 region contralateral to the stimulated paw were: 1.19 ± 0.48%, 1.69 ± 0.21%, 2.47 ± 0.18%, and 2.81 ± 0.37% for 0.5, 1.0, 1.5, and 2.0 mA, respectively. A striking feature of the observed BOLD response (Figs. 3c and 5a, b) is that the signal amplitude started to decay despite ongoing stimulation. The signal maximum was observed typically 30 seconds after stimulation onset, thereafter the amplitude decreased significantly by 5% to 15%. The fitted curves (Fig. 5a) were computed assuming single exponential signal build-up and decay with parameters described in the Materials and Method section. The exponentially decaying vasodilatory response of the neuronal signal is characterized by a time constant $k_v = 0.02\ s^{-1}$. For the build-up of the BOLD signal the same initial rate $k_{on} = 0.002\ s^{-1}$ was assumed, irrespective of the stimulation amplitude applied. In contrast, the value for the decay rate constant k_{off} was found to decrease with increasing stimulation amplitude. This is also apparent when normalizing individual BOLD signals to the respective maximum intensity value (Fig 5b). Single exponential fitting for the averaged curves yielded first-order rate constants of k_{off} values of $0.040\ s^{-1}$ for 2.0 mA, $0.051\ s^{-1}$ for 1.5 mA and $0.063\ s^{-1}$ for 1.0 mA, displaying a linear dependence on the stimulation amplitude with a correlation factor of $R^2 = 1.00$ (data not shown). In the next step we tested whether the decay rate k_{off} depended on the maximal BOLD change. We therefore used the average BOLD signals of all stimulation cycles (four stimulation blocks per stimulation amplitude), which fulfilled the criteria with at least four data points exceeding the noise level used for the fitting procedure (Fig. 5c): a significant negative correlation has been found with $R^2 = 0.76$.

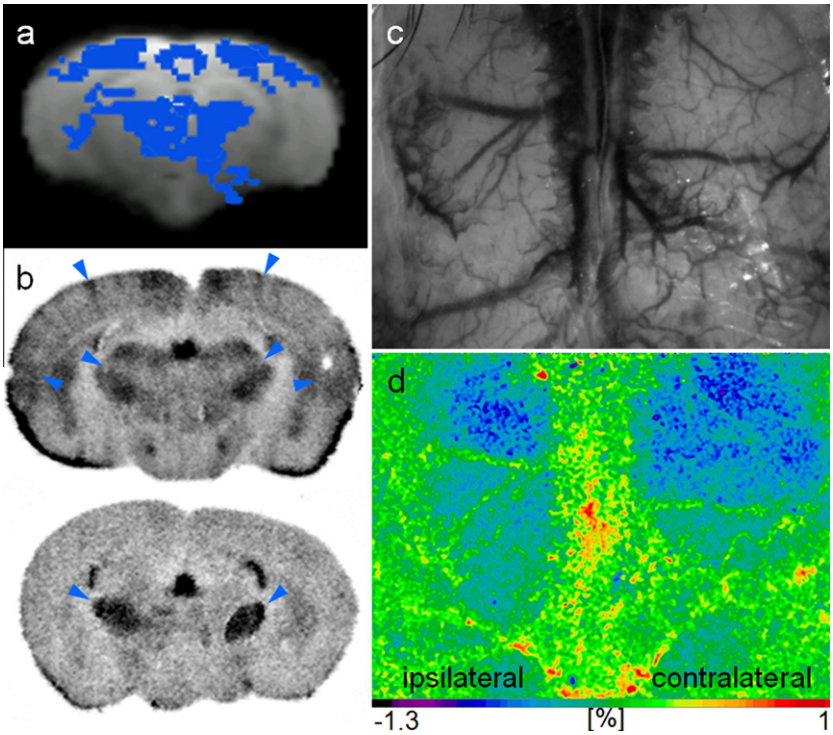

Fig. 6. Autoradiography and intrinsic optical imaging. (a) fMRI activation map of a representative animal. (b) ^{18}F-FDG autoradiographies of two mice after unilateral forepaw stimulation show bilateral thalamic activation and some bilateral cortical activation (blue arrows). (c) Reflection of 570 nm light used for intrinsic optical imaging reveals the vascular anatomy at both sides of the sagittal sinus. (d) Activation map of intrinsic optical imaging shows bilateral activation of the somatosensory area. Regions with increased cerebral blood volume are recognized by a decrease in signal intensity (blue). Color bar indicates changes in signal intensity in [%].

3.7. Autoradiography and intrinsic optical measurements

The autoradiography data of the two animals (Fig. 6b) showed a clear bilateral increase in FDG uptake in the thalamus, consistent with the observed fMRI activation pattern (Fig. 6a). Cortical activation was found to be weak. Bilateral local increases in cortical blood volume indicative of neuronal activation were detected using intrinsic optical imaging (Fig 6d), which is in line with our fMRI finding of bilateral cortical activation.

4. Discussion

fMRI in rodents, predominantly in rats, has become an important tool in biomedical research e.g. to phenotype animal models of CNS disorders [31,32,36,37]. In view of the many genetically engineered mouse lines the development of robust procedures for mouse fMRI protocols should be rewarding. By exploiting the significant gain in sensitivity provided by the use of a cryogenic RF surface coil for signal detection [3,35], BOLD fMRI data sets of high quality suitable for reproducible quantitative analyses have been obtained. The CryoProbe enabled fMRI at a spatial resolution of $200 \times 200 \times 500\ \mu m^3$, which is sufficient to resolve the major cerebral structures of the mouse brain and allows for detailed anatomical and functional studies.

The obtained fMRI data were highly reproducible with regard to both spatial extent and temporal profile. This allowed reliable detection of even small changes in the BOLD amplitude in response to stimulations at different current amplitudes. The BOLD intensity increased significantly at each stimulus onset, though there was a net decrease of BOLD amplitude for subsequent stimulation periods across the cycle consisting of four blocks. This was observed before [18,42] and might be due to adaptation or habituation mechanisms, occurring either peripherally in the stimulated paw, or centrally in the brain. These mechanisms may also contribute to the signal decrease observed during ongoing stimulation (Fig. 3a, b).

Due to the lack of clear evidence whether stimulation was noxious or not, the parameters used were tested on a human subject under the presumption that the threshold to activate C- or Aδ-fibers is similar in humans and mice. However, as the innervation pattern differs, the human values cannot be translated directly to the mouse but should rather be used as an estimate of the noxious threshold. This stands in contrast to a study by Nair and Duong, which reports hind paw stimulation with amplitudes up to 7 mA to be somatosensory only [33]. To our experience, the stimulation used in that study was likely to be noxious, at least at higher amplitudes.

Data analysis revealed a robust activation of the S1 cortical forelimb area. However, the signal was not confined to the S1 region contralateral to the stimulated paw, but was also observed on the ipsilateral side with essentially the same amplitude and spatial extent. This stands in contrast to the majority of fMRI studies in healthy rats which report strictly unilateral responses during unilateral electrical stimulation [15,20,41,53] including our own study using isoflurane anesthesia [48]. We performed additional experiments to modulate the laterality of the fMRI response: varying anesthesia depths, male instead of female mice, or preparing only one paw with electrodes to prevent possible crosstalk between the leads carrying the needle electrodes. None of these interventions affected the bilateral symmetry of the activation pattern observed (data not shown). In addition, electrical forepaw stimulation at 1.5 mA in another strain (HsdWin:NMRI) showed the same bilateral activation pattern (data not shown). Bilateral activation of the areas responsible for pain processing has also been observed

in humans [45–47,49,52]. These bilateral signals may be conveyed by fibers of the corpus callosum [29] or by commissural neurons of the spinal cord [38]. The occurrence of bilateral activation has also been reported previously for rat studies [25]. However, due to our relatively slow temporal resolution of 7.5 s, we were not able to resolve a possible delay between the onset of activation in the two hemispheres. Even increasing the temporal resolution to 1 s was not sufficient to reveal a potential delay of the ipsilateral versus the contralateral activation (data not shown).

Although carried out with a small number of animals, autoradiography and intrinsic optical imaging experiments support our fMRI findings. Autoradiography revealed a distinct bilateral activation of the thalamus, most pronounced in the ventral posterior nuclei, structures known to relay nociceptive information. One mouse also showed bilateral cortical activation in the regions of S2, insula and motor cortex. The intrinsic optical measurement showed a clear bilateral activation of similar amplitudes in both hemispheres. These experiments, which were performed independently from our fMRI setup, are in line with the results obtained with BOLD fMRI.

Besides the S1 region, bilateral activation was observed in the thalamus, the motor, S2 and insular cortex. These regions are known to be part of the nociceptive network. Motor cortex activation might originate from antidromic stimulation of the efferent motor fibers as seen in a study by Cho and colleagues [9]. These activated areas are in accordance with those reported for similar studies in rats [53].

Anesthesia is a recurring issue in animal imaging, in particular when investigating nociception. Isoflurane is an attractive anesthetic as it is easy to administer and control; however, there are also drawbacks. Isoflurane is a potent vasodilator causing a global increase of cerebral blood flow (CBF) in a dose-dependent manner [27]. The basal energy level as derived from the cerebral metabolic rate of glucose consumption (CMR_{glc}) is lower than in the awake state. A reduction by approximately 40% was reported for an isoflurane concentration of 1.4% [22]. In comparison, α-chloralose was found to reduce baseline CMR_{glc} by approximately 60% [25]. The higher energy consumption, the high CBF and concomitantly the dilated vessels in isoflurane-anesthetized animals during baseline conditions reduce the dynamic range of the hemodynamic response as compared to α-chloralose anesthesia [10,19]. The vasodilatory effects however are dose dependent and can therefore be significantly reduced by using relatively low isoflurane levels (at around 1%). At this low level we assume reduced antinociceptive efficacy of isoflurane. Deady et al. showed that the hypnotic effects of isoflurane occurred at lower concentrations than the antinociceptive effects [12]. Also, low concentrations of isoflurane appear to exhibit minimal neuro-suppressive effects, as the flow-metabolism coupling was shown to remain preseved [16]. The robust BOLD response reported in this study as well as data from other studies performed under isoflurane anesthesia prove it to be a useful anesthetic for fMRI studies in rodents [32,33,36,37,40,43].

A recent study [1] performed on mice using electrical forepaw stimulation claims the α2-adrenergic receptor agonist medetomidine to be better for long time studies than other anesthetics. However, the occurrence of BOLD activation in less than 60% of all scans performed (our study: >95%) and the noisy temporal BOLD profiles do not clearly show the superiority of medetomidine anesthesia.

When analyzing the temporal BOLD profile, it became obvious that it consists of two components, of which one is in phase with the stimulation (component *F*), while the other one is much slower, starting with the onset of the first stimulation (component *S*). The two components might be explained in terms of the underlying physiological processes: Component *F* being in phase with the stimulation episodes is probably associated with the peripheral neuronal input of the A and C fibers, while the underlying signal described by component *S* might reflect a slow vascular response.

The BOLD signal amplitude of both components depended linearly on the stimulation amplitude. A similar linear dependence has been demonstrated using cerebral blood volume (CBV) [31] and CBF [42] measurements in mice and rats, respectively. Torebjörk et al. also showed that nociceptor responses and individual pain ratings in humans both linearly correlated with the applied heat stimulation [51].

By averaging and normalizing the BOLD signal curves of all animals, it became apparent that the rate of the signal decay following a stimulation episode decreased with increasing stimulation amplitudes. Stimulation at high amplitudes led to a larger BOLD response and thus to a higher content of oxyhemoglobin (and correspondingly a lower concentration of deoxyhemoglobin) in the vessels, as compared to stimulations at lower amplitudes. This is in line with the hemodynamic model described by Friston and colleagues [14], which combines the balloon model with a linear dynamic model of changes in CBF as caused by neuronal activity. The balloon model describes the link between CBF and the BOLD signal and is able to predict nonlinear effects of the BOLD signal, which contrast the linear relationship of CBF and synaptic activity. The central concept of the model is to treat the venous compartment as an expandable balloon, which is inflated by an increase in CBF, leading to a dilution of the deoxygenated blood and an increased expelling rate of the blood [4]. The model predicts the recovery rate following a stimulation episode to be proportional to the amount of deoxyhemoglobin in the vessel [5,14,4], which is in line with our experimental results (Fig. 5). In contrast, the initial rate of the build-up of the BOLD response was found independent on the current amplitude within error limits.

A further aspect that becomes apparent from the temporal profile of the BOLD response is that the BOLD amplitude decays during stimulation despite ongoing peripheral input. This can be explained by a decaying vasodilatory signal, which is also subject to feedback regulation by CBF, in response to a prolonged neuronal stimulus [15,45]. The neuronal input is described as an initial peak followed by a decay to a lower level [14,4].

We could demonstrate that reproducible mouse BOLD fMRI data can be obtained following sensory stimulation. The high quality of the data and the use of isoflurane make longitudinal fMRI studies in mice feasible.

Conflict of interest statement

None declared.

Acknowledgments

The authors thank the NCCR Neural Plasticity and Repair and the Swiss National Science Foundation for funding this project. There are no conflicts of interest to declare.

References

[1] Adamczak JM, Farr TD, Seehafer JU, Kalthoff D, Hoehn M. High field BOLD response to forepaw stimulation in the mouse. NeuroImage 2010;51:704–12.
[2] Ahrens ET, Dubowitz DJ. Peripheral somatosensory fMRI in mouse at 11.7 T. NMR Biomed 2001;14:318–24.
[3] Baltes C, Radzwill N, Bosshard S, Marek D, Rudin M. Micro MRI of the mouse brain using a novel 400 MHz cryogenic quadrature RF probe. NMR Biomed 2009;22:834–42.
[4] Buxton RB, Uludag K, Dubowitz DJ, Liu TT. Modeling the hemodynamic response to brain activation. NeuroImage 2004;23:S220–233.
[5] Buxton RB, Wong EC, Frank LR. Dynamics of blood flow and oxygenation changes during brain activation: the balloon model. Magn Reson Med 1998;39:855–64.
[6] Casey KL. Forebrain mechanisms of nociception and pain: analysis through imaging. Proc Natl Acad Sci USA 1999;96:7668–74.

[7] Caterina MJ, Leffler A, Malmberg AB, Martin WJ, Trafton J, Petersen-Zeitz KR, Koltzenburg M, Basbaum AI, Julius D. Impaired nociception and pain sensation in mice lacking the capsaicin receptor. Science 2000;288:306–13.
[8] Chang C, Shyu B-C. A fMRI study of brain activations during non-noxious and noxious electrical stimulation of the sciatic nerve of rats. Brain Res 2001;897:71–81.
[9] Cho YR, Pawela CP, Li R, Kao D, Schulte ML, Runquist ML, Yan JG, Matloub HS, Jaradeh SS, Hudetz AG, Hyde JS. Refining the sensory and motor ratunculus of the rat upper extremity using fMRI and direct nerve stimulation. Magn Reson Med 2007;58:901–9.
[10] Corfield DR, Murphy K, Josephs O, Adams L, Turner R. Does hypercapnia-induced cerebral vasodilation modulate the hemodynamic response to neural activation? NeuroImage 2001;13(6 Pt 1):1207–11.
[11] Davis KD, Taylor SJ, Crawley AP, Wood ML, Mikulis DJ. Functional MRI of pain- and attention-related activations in the human cingulate cortex. J Neurophysiol 1997;77:3370–80.
[12] Deady JE, Koblin DD, Eger II EI, Heavner JE, D'Aoust B. Anesthetic potencies and the unitary theory of narcosis. Anesth Analg 1981;60:380–4.
[13] Franklin K, Paxinos G. The mouse brain in stereotaxic coordinates. San Diego: Academic Press; 1997.
[14] Friston KJ, Mechelli A, Turner R, Price CJ. Nonlinear responses in fMRI: the balloon model, volterra kernels, and other hemodynamics. NeuroImage 2000;12:466–77.
[15] Goloshevsky AG, Silva AC, Dodd SJ, Koretsky AP. BOLD fMRI and somatosensory evoked potentials are well correlated over a broad range of frequency content of somatosensory stimulation of the rat forepaw. Brain Res 2008;1195:67–76.
[16] Hansen TD, Warner DS, Todd MM, Vust LJ. The role of cerebral metabolism in determining the local cerebral blood flow effects of volatile anesthetics: evidence for persistent flow-metabolism coupling. J Cereb Blood Flow Metab 1989;9:323–8.
[17] Harvey RJ, Depner UB, Wassle H, Ahmadi S, Heindl C, Reinold H, Smart TG, Harvey K, Schutz B, Abo-Salem OM, Zimmer A, Poisbeau P, Welzl H, Wolfer DP, Betz H, Zeilhofer HU, Muller U. GlyRα3: an essential target for spinal PGE2-mediated inflammatory pain sensitization. Science 2004;304:884–7.
[18] Hsu EW, Hedlund LW, MacFall JR. Functional MRI of the rat somatosensory cortex: effects of hyperventilation. Magn Reson Med 1998;40:421–6.
[19] Kemna LJ, Posse S. Effect of respiratory CO(2) changes on the temporal dynamics of the hemodynamic response in functional MR imaging. NeuroImage 2001;14:642–9.
[20] Kida I, Yamamoto T. Stimulus frequency dependence of blood oxygenation level-dependent functional magnetic resonance imaging signals in the somatosensory cortex of rats. Neurosci Res 2008;62:25–31.
[21] Ledent C, Valverde O, Cossu G, Petitet F, Ccedil, ois, Aubert J-F, Beslot F, oise, ouml , hme GA, Imperato A, Pedrazzini T, Roques BP, Vassart G, Fratta W, Parmentier M. Unresponsiveness to cannabinoids and reduced addictive effects of opiates in CB1 receptor knockout mice. Science 1999;283:401–4.
[22] Lenz C, Rebel A, van Ackern K, Kuschinsky W, Waschke KF. Local cerebral blood flow, local cerebral glucose utilization, and flow-metabolism coupling during sevoflurane versus isoflurane anesthesia in rats. Anesthesiology 1998;89:1480–8.
[23] Lilja J, Endo T, Hofstetter C, Westman E, Young J, Olson L, Spenger C. Blood oxygenation level-dependent visualization of synaptic relay stations of sensory pathways along the neuroaxis in response to graded sensory stimulation of a limb. J Neurosci 2006;26:6330–6.
[24] Linden Avd, Camp Nv, Ramos-Cabrer P, Hoehn M. Current status of functional MRI on small animals: application to physiology, pathophysiology, and cognition. NMR Biomed 2007;20:522–45.
[25] Maandag NJ, Coman D, Sanganahalli BG, Herman P, Smith AJ, Blumenfeld H, Shulman RG, Hyder F. Energetics of neuronal signaling and fMRI activity. Proc Natl Acad Sci USA 2007;104:20546–51.
[26] Manning BH, Morgan MJ, Franklin KB. Morphine analgesia in the formalin test: evidence for forebrain and midbrain sites of action. Neuroscience 1994;63:289–94.
[27] Matta BF, Heath KJ, Tipping K, Summors AC. Direct cerebral vasodilatory effects of sevoflurane and isoflurane. Anesthesiology 1999;91:677–80.
[28] Millan MJ. The induction of pain: an integrative review. Prog Neurobiol 1999;57:1–164.
[29] Mohajerani MH, McVea DA, Fingas M, Murphy TH. Mirrored bilateral slow-wave cortical activity within local circuits revealed by fast bihemispheric voltage-sensitive dye imaging in anesthetized and awake mice. J Neurosci 2010;30:3745–51.
[30] Morrow TJ, Paulson PE, Danneman PJ, Casey KL. Regional changes in forebrain activation during the early and late phase of formalin nociception: analysis using cerebral blood flow in the rat. Pain 1998;75:355–65.
[31] Mueggler T, Baumann D, Rausch M, Staufenbiel M, Rudin M. Age-dependent impairment of somatosensory response in the amyloid precursor protein 23 transgenic mouse model of alzheimer's disease. J Neurosci 2003;23:8231–6.
[32] Mueggler T, Sturchler-Pierrat C, Baumann D, Rausch M, Staufenbiel M, Rudin M. Compromised hemodynamic response in amyloid precursor protein transgenic mice. J Neurosci 2002;22:7218–24.
[33] Nair G, Duong TQ. Echo-planar BOLD fMRI of mice on a narrow-bore 9.4 T magnet. Magn Reson Med 2004;52:430–4.
[34] Nassar MA, Stirling LC, Forlani G, Baker MD, Matthews EA, Dickenson AH, Wood JN. Nociceptor-specific gene deletion reveals a major role for Nav1.7 (PN1) in acute and inflammatory pain. Proc Natl Acad Sci USA 2004;101:12706–11.
[35] Ratering D, Baltes C, Nordmeyer-Massner J, Marek D, Rudin M. Performance of a 200-MHz cryogenic RF probe designed for MRI and MRS of the murine brain. Magn Reson Med 2008;59:1440–7.
[36] Reese T, Bjelke B, Porszasz R, Baumann D, Bochelen D, Sauter A, Rudin M. Regional brain activation by bicuculline visualized by functional magnetic resonance imaging. Time-resolved assessment of bicuculline-induced changes in local cerebral blood volume using an intravascular contrast agent. NMR Biomed 2000;13:43–9.
[37] Reese T, Bochelen D, Baumann D, Rausch M, Sauter A, Rudin M. Impaired functionality of reperfused brain tissue following short transient focal ischemia in rats. Magn Reson Imaging 2002;20:447–54.
[38] Ruscheweyh R, Sandkühler J. Long-range oscillatory Ca^{2+} waves in rat spinal dorsal horn. Eur J NeuroSci 2005;22:1967–76.
[39] Sanganahalli BG, Bailey CJ, Herman P, Hyder F. Tactile and non-tactile sensory paradigms for fMRI and neurophysiologic studies in rodents. Methods Mol Biol 2009;489:213–42.
[40] Sauter A, Reese T, Porszasz R, Baumann D, Rausch M, Rudin M. Recovery of function in cytoprotected cerebral cortex in rat stroke model assessed by functional MRI. Magn Reson Med 2002;47:759–65.
[41] Silva AC, Koretsky AP, Duyn JH. Functional MRI impulse response for BOLD and CBV contrast in rat somatosensory cortex. Magn Reson Med 2007;57:1110–8.
[42] Silva AC, Lee SP, Yang G, Iadecola C, Kim SG. Simultaneous blood oxygenation level-dependent and cerebral blood flow functional magnetic resonance imaging during forepaw stimulation in the rat. J Cereb Blood Flow Metab 1999;19:871–9.
[43] Sommers MG, Egmond Jv, Booij LH, Heerschap A. Isoflurane anesthesia is a valuable alternative for alpha-chloralose anesthesia in the forepaw stimulation model in rats. NMR Biomed 2009;22:414–8.
[44] Spaeth N, Wyss MT, Weber B, Scheidegger S, Lutz A, Verwey J, Radovanovic I, Pahnke J, Wild D, Westera G, Weishaupt D, Hermann DM, Kaser-Hotz B, Aguzzi A, Buck A. Uptake of 18F-fluorocholine, 18F-fluoroethyl-L-tyrosine, and 18F-FDG in acute cerebral radiation injury in the rat: implications for separation of radiation necrosis from tumor recurrence. J Nucl Med 2004;45:1931–8.
[45] Stancák A, Svoboda J, Rachmanová R, Vrána J, Králík J, Tintera J. Desynchronization of cortical rhythms following cutaneous stimulation: effects of stimulus repetition and intensity, and of the size of corpus callosum. Clin Neurophysiol 2003;114:1936–47.
[46] Staud R, Craggs JG, Robinson ME, Perlstein WM, Price DD. Brain activity related to temporal summation of C-fiber evoked pain. Pain 2007;129:130–42.
[47] Sutherland MT, Tang AC. Reliable detection of bilateral activation in human primary somatosensory cortex by unilateral median nerve stimulation. NeuroImage 2006;33:1042–54.
[48] Sydekum E, Baltes C, Ghosh A, Mueggler T, Schwab ME, Rudin M. Functional reorganization in rat somatosensory cortex assessed by fMRI: elastic image registration based on structural landmarks in fMRI images and application to spinal cord injured rats. NeuroImage 2009;44:1345–54.
[49] Terekhin P, Forster C. Hypocapnia related changes in pain-induced brain activation as measured by functional MRI. Neurosci Lett 2006;400:110–4.
[50] Thal SC, Plesnila N. Non-invasive intraoperative monitoring of blood pressure and arterial pCO_2 during surgical anesthesia in mice. J Neurosci Methods 2007;159:261–7.
[51] Torebjork HE, LaMotte RH, Robinson CJ. Peripheral neural correlates of magnitude of cutaneous pain and hyperalgesia: simultaneous recordings in humans of sensory judgments of pain and evoked responses in nociceptors with C-fibers. J Neurophysiol 1984;51:325–39.
[52] Torquati K, Pizzella V, Babiloni C, Gratta CD, Penna SD, Ferretti A, Franciotti R, Rossini PM, Romani GL. Nociceptive and non-nociceptive sub-regions in the human secondary somatosensory cortex: an MEG study using fMRI constraints. NeuroImage 2005;26:48–56.
[53] Tuor UI, Malisza K, Foniok T, Papadimitropoulos R, Jarmasz M, Somorjai R, Kozlowski P. Functional magnetic resonance imaging in rats subjected to intense electrical and noxious chemical stimulation of the forepaw. Pain 2000;87:315–24.
[54] Wilson SG, Mogil JS. Measuring pain in the (knockout) mouse: big challenges in a small mammal. Behav Brain Res 2001;125:65–73.
[55] Wyss MT, Obrist NM, Haiss F, Eckert R, Stanley R, Burger C, Buck A, Weber B. A beta-scintillator for surface measurements of radiotracer kinetics in the intact rodent cortex. NeuroImage 2009;48:339–47.